# OPTIMIZING HORIZONTAL-RESOLUTION IMPROVEMENT OF THE MASW METHOD

*Julian Ivanov, Kansas Geological Survey, Lawrence, Ks*
*Jianghai Xia, Kansas Geological Survey, Lawrence, Ks*
*Richard D. Miller, Kansas Geological Survey, Lawrence, Ks*



## Abstract

The MASW method estimates the shear-wave velocity from the properties of the Rayleigh-wave propagation measured within a seismic spread. Shorter wave-length components of the surface-wave sample the shallow parts of the seismic section and longer wave-length components sample the deeper parts of the earth. The greater the wave-length the greater volumes of the earth affect the surface-wave properties. Thus, the surface-wave results are strongly affected by averaging. Such smearing reduces the horizontal resolution of the shear-wave velocity estimates.

A method developed to increase the horizontal resolution of any geophysical model by using generalized inversion provided encouraging results applied to the MASW Vs results. The existing method is expanded targeting specifically the improvement of the horizontal resolution of the MASW method. Traditionally MASW data is acquired once moving the seismic source and spread at a chosen direction along the line. If the sampling of the surveyed line is performed twice, by moving the source and the receiver spread in both directions along the line, the MASW unblurring technique can be optimized. An optimal unblurring operator is sought for which the two unblurred lines (shot from different directions) would have the best match (would be least different).

Application of the proposed optimized unblurring method on real data did not provide a unique solution for the particular data set. The proposed technique can be a valuable tool for improving the horizontal resolution of the MASW method but also of any other type of overlapping geophysical data set.

## Introduction

The multichannel analysis of surface-wave (MASW) method was developed to estimate near-surface S-wave velocity from high-frequency (≥ 2 Hz) Rayleigh-wave data (Park et al., 1999; Xia et al., 1999a). The practical application of MASW has provided reliable correlations to drill data. Miller et al. (1999a) mapped bedrock with 0.3-m (1-ft) accuracy at depths of about 4.5-9 m (15-30 ft), confirmed by numerous borings. The MASW method has been applied to problems such as characterization of pavements (Park et al., 2001; Ryden et al., 2001), the study of Poisson's ratio (Ivanov et al., 2000a), investigation of sea-bottom sediment stiffness (Park et al., 2000; Ivanov et al., 2000b), detection of dissolution features (Miller et al., 1999b), and measurement of S-wave velocity as a function of depth (Xia et al., 1999b). Studies on the MASW method have been extended to areas of utilization of higher modes (Xia et al., 2003; Beaty et al., 2002; Beaty and Schmitt, 2003), determination of near-surface *Q* (Xia et al., 2002), and deployment of autojuggie (Steeples et al., 1999) with the MASW method (Tian et al., 2003a and 2003b).

The evaluation of the resolution of high-frequency surface-wave data/model remains a research topic. Xia and Chen (2003) proposed a smear-matrix concept, which explained the vertical resolution of S-wave velocity profile resulting from inversion of Rayleigh-wave data. Xia et al. (2004) developed an unblurring technique to improve the horizontal resolution of 2-D S-wave velocity sections obtained by

the MASW method. They obtained encouraging results. However, their method was based on subjectively determined data kernel (a weighting matrix). Thus, it remained unclear if the selected unblurring parameters were optimal for a given data set.

To define optimal unblurring parameters we propose a method, which uses two data sets, shot in different directions along a given 2-D line. The two data sets are unblurred multiple times using a range of unblurring operators (each of which defines the corresponding data kernel). For each data kernel the fitness between the two unblurred images of the two data sets is measured. The optimum inversion (unblurring) parameters would be those for which the two unblurred data set have the best fit (minimal difference).

We were expecting that the proposed 2-fold method would easily provide a data kernel that is optimal for any overlapping two data sets. Testing the optimization technique on real data revealed that for a given data set there might not be a unique solution to the problem. Significantly different data kernels provided similar minimal difference between the unblurred data sets.

***The Unblurring Method***

The unblurring method (Xia et al., 2004) was developed on the basis of the image enhancing technique presented by Menke (1989). It assumed that each image pixel (say, in a camera) was a result of summation of the influence of three neighboring elements (Figure 1).

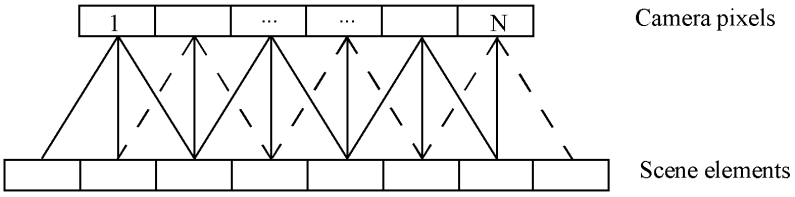


**Figure 1**. When a camera moves through three scene elements during an exposure, each camera pixel records the average brightness of three neighboring scene elements. There are two more unknowns than data (From Menke (1989).

Thus, considering the available image (vector **c**) to be blurred, the blurring can be described by a system of equations **c** = **Gs,** where **s** is the vector of contributing scene elements and **G** is the matrix describing the contribution of each scene element, referred to as the data kernel. Assuming varying contribution from each scene element, the data kernel, **G,** may have the form,

$$\mathbf{G} = \begin{bmatrix} 1 & 0 & 0 & 0 & 0 & \dots & 0 \\ 1/4 & 1/2 & 1/4 & 0 & 0 & \dots & 0 \\ 0 & 1/4 & 1/2 & 1/4 & 0 & \dots & 0 \\ & & & \vdots & & & \\ & & & \vdots & & & \\ 0 & 0 & 0 & 0 & 1/4 & 1/2 & 1/4 \\ 0 & 0 & 0 & 0 & 0 & 0 & 1 \end{bmatrix}.$$

In the above example, blurring is a result of contribution of only three elements and it was assumed that the side element had half the contribution of the central element. The top and bottom extra rows (containing only "1"s) were added to make the system determined, and thus stabilize the inverse

problem. Unblurring is finding the solution (vector **s**) to the system above. More technical details about the unblurring method can be found in Xia et al. (2004).

### *Real-world Example*

The unblurring technique was applied to MASW data acquired in Andalusia, Alabama in 1999 (Miller and Xia, 1999). The data were collected within the Conecuh National Forest, where sinkholes were present, using a 60-channel Geometrics StrataView seismograph with forty-eight 4.5 Hz vertical-component geophones and a weight drop, built in Kansas Geological Survey. Geophone spacing was 4 ft and source locations were at every 8 ft. The nearest offset was 30 ft in an effort to map subsurface down to 100 ft depth. Data were acquired from both directions along the line. Total of 40 shots were collected along each direction, following the CDP roll-along format. After applying the MASW method two 2-D S-wave velocity sections were acquired (Figure 2).

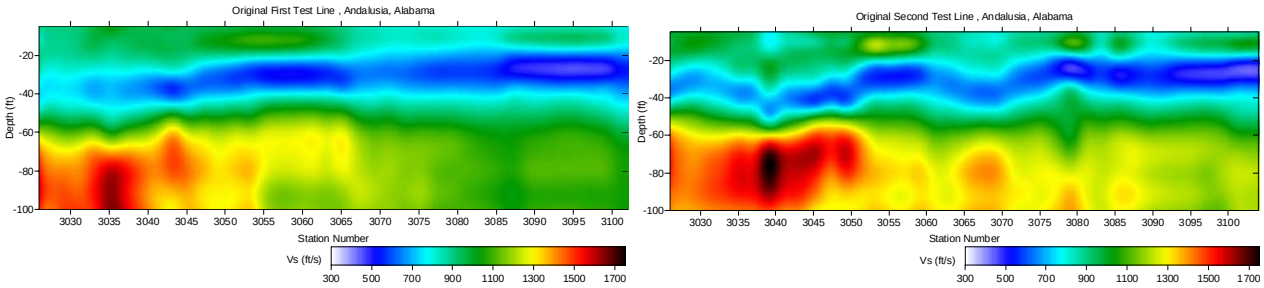


**Figure 2**. First and second 2-D S-wave velocity sections from data acquired in both directions along the line.

To unblur these two images Xia et al. (2004) assumed that each S-wave estimation sample was a result of contribution of 23 elements, with the central element having the largest weight (0.083). The weight linearly decreased toward most distant element (0.0069) (the sum all the weight coefficient equaling to1). Such a 23-element operator defined each row of the data kernel. The inverse unblurring technique was applied on layer-by-layer basis (Figure 3).

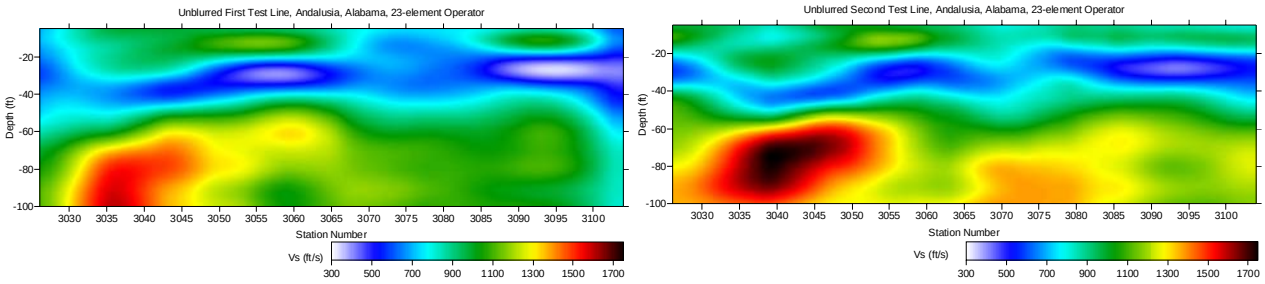


**Figure 3**. Unblurred first and second 2-D S-wave velocity sections using a 23-point operator from data acquired in both directions along the line.

The difference between the two unblurred overlapping sections was smaller than the difference between the original 2-D Vs sections. Therefore, the unblurred solutions were considered to be more realistic than the original 2-D Vs sections.

## Optimizing the Unblurring Method

The necessity to optimize the unblurring method was cause by the fact that the length of the unblurring operator, which formed the data kernel, was subjectively determined. We propose the following algorithm for finding an optimum unblurring operator. All the reasonable range of operator lengths can be used to estimate for each of them a corresponding set of overlapping unblurred sections and their difference measured. The optimum-unblurring operator would be the one that would produce unblurred sections that fit best (have minimal difference). It was expected that this algorithm would provide a strait-forward solution by finding a unique optimum operator that would provide a best fit.

***Real-world Example Continued***

This was not the case with the data set at hand. There are several operator lengths that cause similar minimal difference between the unblurred sections (Figure 4). One is the 23-element operator used originally by Xia et al. (2004). Another is a 3-element operator, which produced unblurred sections (Figure 5) that fit even better bellow 35 ft depth (the left red dashed line on Figure 4).

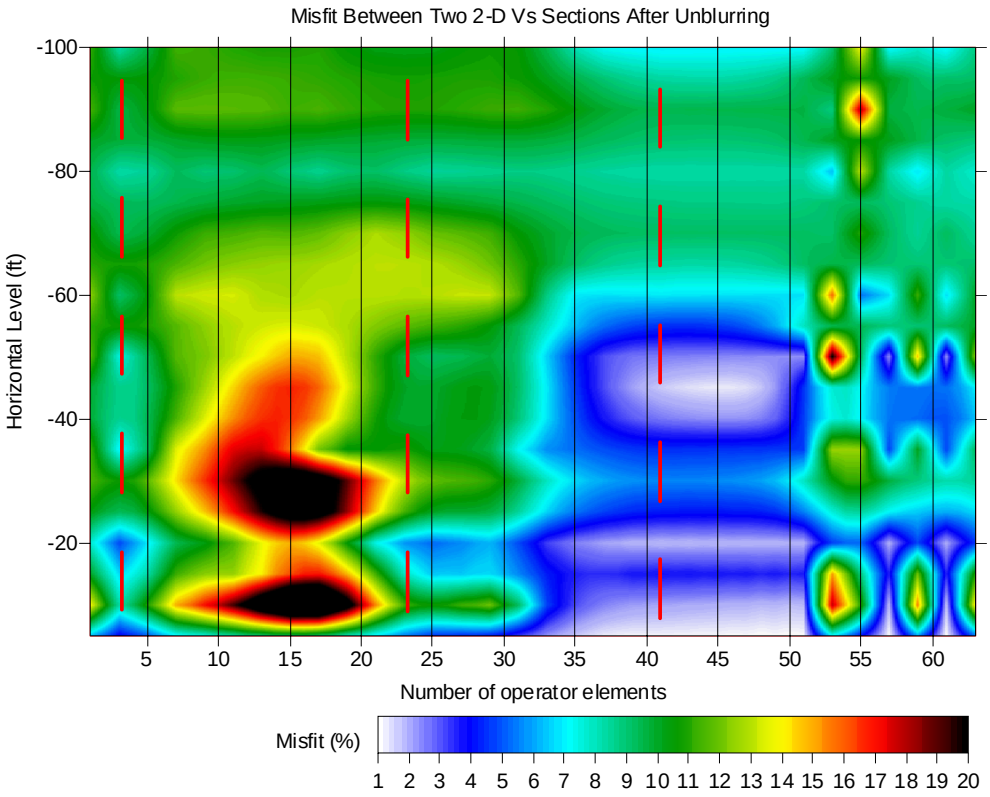


**Figure 4**. Percent mismatch error map. The horizontal axis indicates the unblurring operator length, which forms the data kernel. The vertical axis shows the depth at which the average percent difference between the two overlapping sections was estimated. Red dashed lines show minimal-error regions.

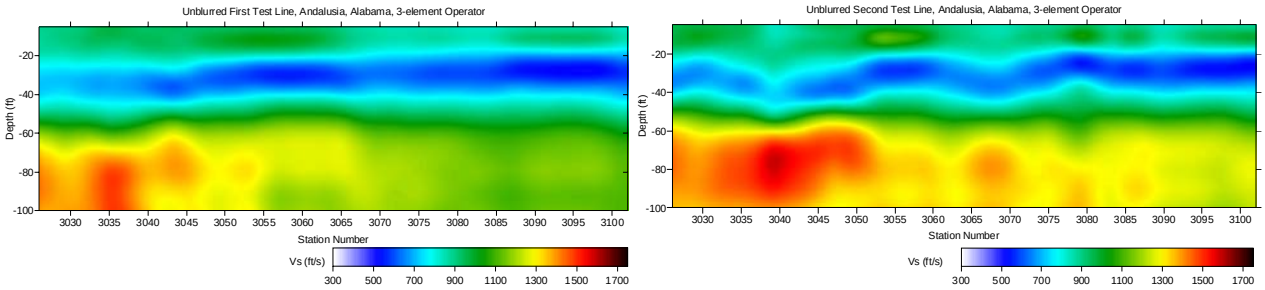


**Figure 5**. Unblurred first and second 2-D S-wave velocity sections using a 3-point operator from data acquired in both directions along the line.

Then there is the 37- to 49-element operator length range with even better fit between the overlapping unblurred sections (Figure 6).

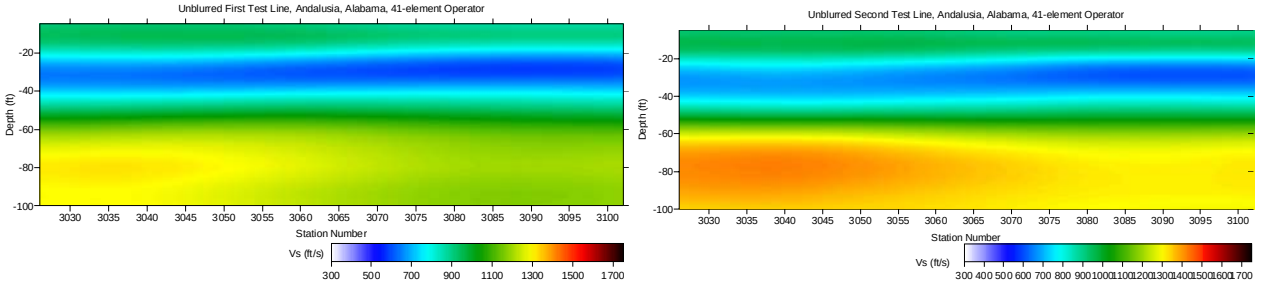


**Figure 6**. Unblurred first and second 2-D S-wave velocity sections using a 41-point operator from data acquired in both directions along the line.

Thus, this optimization attempt did not provide a unique solution for the particular data set. Further considerations of the obtain results suggest that the 37- to 49-element operator length range can be excluded as a place for the possible solution because of its filtered (smeared) results, which are due to numerical artifacts, resulting from the operator length approaching the amount of available data. Currently, it is difficult to give preference to one of the available minimal-error unblurred solutions (Figures 3 and 5). It may seem that the 3-element operator is more likely, because it modifies to a minimal degree the input data and because it provides the best fitness between the two MASW lines. However, taking into account the possibilities for error in the MASW results, the 23-element operator may still be a viable option for the true, optimal operator. Only ground truth (for example, from wells) can resolve the problem.

## Discussion and Conclusions

The optimized unblurring method can be a powerful tool for increasing the horizontal resolution of the MASW method.

The proposed optimized unblurring method cannot guarantee a unique solution, as indicated by tests on real data. However, such nonuniqueness may be related exclusively to a particular data set, which may be result of noise and errors during the application of the MASW method, either during the dispersion curve picking process, either during the inversion stage. Further research on other operator patterns, which fill the data kernel, may improve the optimized unblurring method. Acquiring more overlapping data along the line could allow larger operators to be tested.

The optimized unblurring technique has the potential to be successfully applied to any geophysical data, acquired in both directions along a given line, and thus improve its horizontal resolution.

## References


Beaty, K.S., Schmitt, D.R., and Sacchi, M., 2002, Simulated annealing inversion of multimode Rayleigh wave dispersion curves for geological structure: Geophys. J. Int., **151**, 622–631.

Beaty, K.S., and Schmitt, D.R., 2003, Repeatability of multimode Rayleigh-wave dispersion studies, Geophysics, v. **68**, no. 3, 782-790.

Ivanov, J., Park, C.B., Miller, R.D., and Xia, J., 2000a, Mapping Poisson's Ratio of unconsolidated materials from a joint analysis of surface-wave and refraction events: Proceedings of the Symposium on the Application of Geophysics to Engineering and Environmental Problems, Arlington, Va., February 20-24, 2000.

Ivanov, J., Park, C.B., Miller, R.D., and Xia, J., 2000b, Joint analysis of surface-wave and refracted events from river-bottom sediments: Technical Program with Biographies, SEG, 70th Annual Meeting, Calgary, Alberta, Canada, 1307-1310.

Menke, W., 1989, Geophysical data analysis: Discrete inverse theory: Academic Press Inc., 37, 38, 48, 62, 65, 152, 153, 155.

Miller, R.D., and Xia, J., 1999, Feasibility of seismic techniques to delineate dissolution features in the upper 600 ft at Alabama Electric Cooperative's proposed Damascus site, Interim Report: Kansas Geological Survey Open-file Report 99-3.

Miller, R. D., Xia, J., Park, C. B., and Ivanov, J.M., 1999a, Multichannel analysis of surfaces waves to map bedrock: Leading Edge, **18**, 1392-1396.

Miller, R., Xia, J., Park, C., Davis, J., Shefchik, W., and Moore, L., 1999b, Seismic techniques to delineate dissolution features in the upper 1000 ft at a power plant: Technical Program with Biographies, SEG, 69th Annual Meeting, Houston, Texas, 492-495.

Park, C. B., Ivanov, J., Miller, R. D., Xia, J., and Ryden, N., 2001, Multichannel analysis of surface waves (MASW) for pavement: Feasibility test: 5th SEGJ Int. Symposium, Tokyo, Japan, January 24-26, 2001.

Park, C.B., Miller, R.D., Xia, J., and Ivanov, J., 2000, Multichannel analysis of underwater surface wave near Vancouver, B.C., Canada: Technical Program with Biographies, SEG, 70th Annual Meeting, Calgary, Alberta, Canada, 1303-1306.

Park, C. B., Miller, R. D., and Xia, J., 1999, Multichannel analysis of surface waves: Geophysics, **64**, 800-808.

Ryden, N., Park, C., Miller, R., Xia, J., and Ivanov, J., 2001: High frequency MASW for non-destructive testing of pavements: Proceedings of the Symposium on the Application of Geophysics to Engineering and Environmental Problems, Denver, Colorado, March 4-7, 2001.

Steeples, D.W., Baker, G.S., and Schmeissner, C., 1999, Toward the autojuggie: Planting 72 geophones in 2 sec: Geophysical Research Letters, 26, 1085-1088.

Tian, G., Steeples, D.W., Xia, J., Miller, R.D., Spikes, K.T., and Ralston, M.D., 2003a, Multichannel analysis of surface wave method with the autojuggie: Soil Dynamics and Earthquake Engineering, v. 23, no. 3, 243-247.

Tian, G., Steeples, D.W., Xia, J., and Spikes, K.T., 2003b, Useful resorting in surface wave method with the autojuggie: Geophysics, v. 68, no. 6, 1906-1908.

Xia, J., R.D. Miller, C. Chen, and J. Ivanov, 2004, Increasing horizontal resolution of geophysical models by generalized inversion [Exp. Abs.]: Soc. Expl. Geophys., p. 1437-1440

Xia, J., and Chen, C., 2003, Model resolution of gross Rayleigh wave data: Technical Program with Biographies, SEG, 73rd Annual Meeting, Dallas, TX, 1243-1246.

Xia, J., Miller, R.D., Park, C.B., and Tian, G., 2003, Inversion of high-frequency surface waves with fundamental and higher modes: Journal of Applied Geophysics, v. **52**, no. 1, 45-57.

Xia, J., Miller, R.D., Park, C.B., and Tian, G., 2002, Determining Q of near-surface materials from Rayleigh waves: Journal of Applied Geophysics, v. **51**, no. 2-4, 121-129.

Xia, J., Miller, R.D., and Park, C.B., 1999a, Estimation of near-surface shear-wave velocity by inversion of Rayleigh wave: Geophysics, **64**, 691-700.

Xia, J., Miller, R. D., Park, C. B., Hunter, J. A., and Harris, J. B., 1999b, Evaluation of the MASW technique in unconsolidated sediments: 69th Ann. Mtg., Soc. Expl. Geophys., Expanded Abstracts, 437-440.

## Acknowledgments

The authors would like to thank Mary Brohammer for her assistance in manuscript preparation and submission.